analytical chemistry

pubs.acs.org/ac Article

Enzyme-Catalyzed Hydrolysis of Lipids in Immiscible Microdroplets Studied by Contained-Electrospray Ionization

Benjamin J. Burris and Abraham K. Badu-Tawiah*

Cite This: *Anal. Chem.* 2021, 93, 13001−13007 Read Online

ACCESS | Metrics & More | Article Recommendations | Supporting Information

ABSTRACT: Enzyme-catalyzed hydrolysis of lipids was monitored directly in immiscible microdroplet environments using contained-electrospray mass spectrometry. Aqueous solution of the lipase enzyme from *Pseudomonas cepacia* and the chloroform solution of the lipids were sprayed from separate capillaries, and the resultant droplets were merged within a reaction cavity that is included at the outlet of the contained-electrospray ionization source. By varying the length of the reaction cavity, the interaction time between the enzyme and its substrate was altered, enabling the quantification of reaction product as a function of time. Consequently, enhancement factors were estimated by comparing rate constants derived from the droplet experiment to rate constants calculated from solution-phase conditions. These experiments showed enhancement factors greater than 100 in favor of the droplet experiment. By using various lipid types, two possible mechanisms were identified to account for lipase reactivity in aerosols: in-droplet reactions for relatively highly soluble lipids and a droplet coalescence mechanism that allows interfacial reactions for the two immiscible systems.

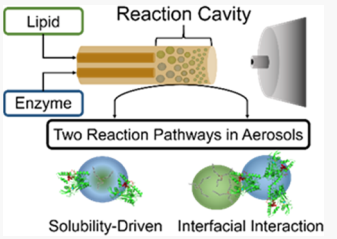

INTRODUCTION

The sea surface microlayer (SSML; thickness 1−1000 μm)[1] is home to diverse groups of marine neuston of which bacteria is the most abundant domain, forming approximately 70% of the total biomass in surface waters.[2] The SSML is a dynamic chemical system subject to various nonequilibrium processes different from that in subsurface water. For example, while lipids and other organic matter are known to be enriched in the upper ocean due to surface activity,[3−6] phytoplankton-derived particulates such as the polysaccharidic transparent exopolymer particles (TEPs) are far more abundant in SSML.[4,7] The intimate association of TEP with microbial life (*e.g.*, through physical support) has been described, including the fact that TEP creates a less diffusive microenvironment (via gelatinous film formation) at the sea surface that effectively supports biochemical reactions such as enzymatic hydrolysis of biopolymers (including TEP itself).[8] Such enzymatic reactions are not only enhanced in SSML but also contribute to the dynamic nature of the SSML by the formation of smaller chemical species, some of which are constantly released into the atmosphere.[8] For example, the enrichment of extracellular carbonic anhydrase in the SSML has been shown to enhance air−sea CO_2 exchange by 15%.[9]

Aside from selective liberation of volatile organic compounds from the SSML, perturbations in the ocean (e.g., via crashing waves) transfer nonvolatile entities (bacteria, viruses, and free enzymes, among others)[10−12] into the atmosphere in the form of sea spray aerosols (SSAs). The specific compositions of the SSAs play profound roles in the chemistry of the environment and subsequent climate changes.[13,14] Like their SSML precursor, SSAs are not static entities. Throughout the day, aerosol composition is highly variable due to the changing composition of atmospheric gases.[15,16] The specific time of the year and source location of the SSAs can determine aerosol composition, for example, due to algal blooms.[14,17−19] Through controlled laboratory experiments, and the use of coastal marine aerosols collected in the field,[20] Malfatti and coworkers recently demonstrated that the activities of enzymes such as lipases, proteases, and alkaline phosphatases are increased in SSA by about 2 orders of magnitude compared with enzymatic activity measured for bulk seawater.

Although other previous studies have examined aerosol size and composition, using online instruments such as aerosol mass spectrometers and aerosol time-of-flight mass spectrometers,[21,22] the studies by Malfatti, which utilized offline fluorescence measurements established, for the first time, a facile biotic pathway that can change the chemical composition of marine aerosols after ejection from the ocean. The use of fluorescence to evaluate enzyme activity requires dissolution of the collected aerosols into solution, a process that makes it difficult to distinguish actual enhancement in the aerosol from concentration effects associated with the collection process. Take the reaction between lipase and lipid substrates (*e.g.*, triolein) as an example, where two immiscible phases are involved. The lipase is soluble in aqueous media, but it has been shown to exhibit high stability in the presence of various

Received: July 2, 2021
Published: September 15, 2021

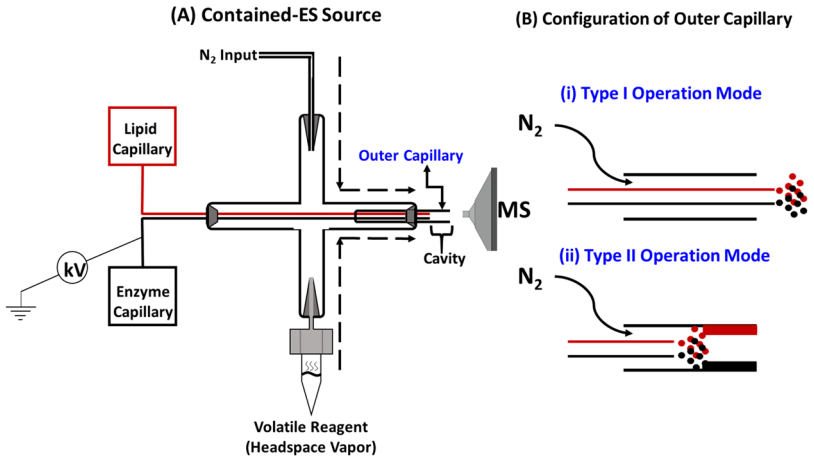

Figure 1. (A) Coaxial contained-electrospray (ES) ionization apparatus having four inputs: delivery of enzyme and lipid solutions via ES emitters, nebulizer gas, and headspace vapor. These inputs converge in an outer capillary in which the two ES emitters are inserted. (B) Outlet for the four inputs can be configured to operate in two distinct modes: (i) type I and (ii) type II spray modes where the ES capillaries protrude or regress, respectively, to control the residence time of reactants in the droplets. In type II operation mode, a thin film can form (noted by thick black/red lines) with thickness approximately 20−30 μm at a 100 psi nebulizer gas pressure.[31] Further details are discussed in the Supporting Information.

organic solvents.[23] For reactions in SSML, the lipase is thought to insert itself in the organic phase with the active site open to the lipid substrate.[24] This mechanism could be different for microliter size aerosols where competition for surface can cause the opposite effect. Aerosol-specific mass spectrometers can be beneficial in this regard, but these instruments suffer from a lack of specificity, limiting the ability to distinguish the different sources of free fatty acid, including those produced by enzymatic reactions. We present here an ambient mass spectrometry (MS) experiment for studying enzymatic reactions in droplets at atmospheric pressure. While it is customary in the atmospheric community to discuss particles of certain sizes as "aerosols", it is conventional to refer to the particles produced via electrospray as "droplets" or "micro-droplets".

Chemicals. Lipids (glyceryl trioleate [triolein], glyceryl trilinoleate [linolein], L-α-phosphatidylethanolamine, dioleoyl [PE-dioleoyl]), lipase (lipase from *Pseudomonas cepacia*), and Tris−ethylenediaminetetraacetic acid (EDTA) buffer solution (pH 8) were obtained from Sigma-Aldrich (St. Louis, MO). Chloroform was obtained from Mallinckrodt Baker, Inc. (Paris, KY). Unless otherwise noted (specifically for environmental conditions), lipid and lipase solutions were prepared to be approximately 25 μM.

EXPERIMENTAL METHODS

Contained-Electrospray Platform. The contained-electrospray ionization (ESI) platform was constructed using a Swagelok cross-junction outside diameter (1/16″ tube OD) (Solon, Ohio (OH)). Sheath gas input was created using a Swagelok stainless steel reducing union (1/4″ × 1/16″ tube OD). The polypropylene headspace vapor container was lodged within a stainless steel Swagelok nut (5/16″ tube OD). To transfer the aqueous solution of lipase and the organic solution of lipid in the droplet phase, a union assembly polyether ether ketone (PEEK) connector was employed to connect syringes to capillaries. The solution of the enzyme and the lipid was delivered individually through deactivated fused silica capillaries (ID 0.10 mm), as illustrated in Figure 1A. The two capillaries were inserted into a larger fused silica outer capillary (ID 0.45 mm, length 15 mm) (Agilent Technologies, Santa Clara, CA), which provides a reaction cavity of variable length. Capillaries were held in place using graphite ferrules (Restek, Bellefonte, PA).

Mass Spectrometry. Mass spectra were collected using a Thermo Fisher Scientific Velos Pro ion trap mass spectrometer (San Jose, CA). The outermost emitter was kept a constant distance away from the mass spectrometer inlet (5 mm). Experimental parameters for MS analyses were solvent flow rate: 5 μmL/min; spray voltage: 5 kV. The MS parameters were 200 °C capillary temperature; 3 microscans; 100 ms ion injection time. Spectra were recorded for at least 30 s.

To probe the bulk reaction, we first performed preliminary experiments in which samples were collected from the aqueous phase, the organic phase, and at the interface between the two phases. We determined that the interface contained the greatest concentration of free fatty acid at all reaction time studies. Therefore, the interface between the aqueous phase and the organic phase was carefully probed for the kinetic studies. Solutions sampled from the interface were analyzed by electrospray ionization mass spectrometry (ESI-MS) to determine the amount of fatty acid produced by the enzyme hydrolysis. To eliminate the immiscibility between lipase and lipid solutions, solutions were created using methanol/water and methanol/chloroform mixtures. Both lipid and lipase were, at concentrations relevant to this study, insoluble in pure methanol, so a water/methanol (1:1, v/v) mixture was used for the lipase and a chloroform:methanol (1:2, v/v) mixture was used for the lipid. Upon mixing (in bulk), this created a homogeneous mixture.

RESULTS AND DISCUSSION

Online Reaction with Contained-Electrospray. We sought to create aerosol proxies using contained-electrospray (Figure 1A) to evaluate enzymatic reactions directly in the aerosol environment. Proteins are known to maintain native-like structures and enzymatic activity when sprayed via electrospray.[25−27] Lipase catalyzes the breakdown of lipids into individual fatty acids. The fatty acid products being surface-active have implications not only in atmospheric chemistry but also in their detection, for example, by electrospray ionization (ESI) mass spectrometry (MS). We

https://doi.org/10.1021/acs.analchem.1c02785
Anal. Chem. 2021, 93, 13001−13007

chose to study the reactivity of the lipase toward three different lipids: glyceryl trioleate (triolein, MW 885 Da), glyceryl trilinoleate (linolein, MW 879 Da), and L-α-phosphatidylethanolamine dioleoyl (PE-dioleoyl, MW 743 Da). The lipids were prepared in chloroform, which was observed to favorably support ionization (see Figure S1). As part of our ongoing research in the development of contained ion sources,[28−32] the current study represents that first time we have employed the coaxial spray mode where two spray capillaries deliver two liquid-phase reagents individually into the reaction cavity, the variable length of which allowed for customized mixing times between reagents (see the Supporting Information for details regarding the construction of the coaxial contained-electrospray (ES) platform). Recent experiments investigating the spray dynamics of the contained-ES source have shown that liquid reagents are first delivered into the reaction cavity as thin films, which are then dispersed into slow-moving (velocity of ∼10 mm/s) bulky droplets (average size 25 μm) upon nebulization with 100 psi N_2 gas. The specific time the droplets spend in the cavity can be controlled by changing the length of the reaction cavity and pressure of the nebulizer gas.[31] This spray condition, where reagents are delivered into a cavity to reduce droplet speed to enhance reactivity, is referred to as the type II operation mode (Figure 1B,ii). By pushing the electrospray capillaries out of the cavity, the operation mode of the contained-ES source is changed to type I (Figure 1B,i), where the enzyme and its substrate are mixed through droplet fusion in ambient air. Droplet speed is approximately 100 m/s in the type I operation mode at a 100 psi N_2 pressure,[33,34] signifying that minimal mixing of reagent occurs compared with the type II operation mode. These distinct spray modes allow us to change the residence time of the lipase in the aerosol environment from millisecond (type I mode) to second (type II mode) time scales. The modified droplets containing reaction products are transferred to a proximal mass spectrometer for chemical characterization.

Hydrolysis of Lipids. The hydrolysis of the lipid triolein by lipase is illustrated in Figure 2A in which three molecules of oleic acid (MW 282 Da) are released alongside the glycerol backbone. Three similar lipids were selected to examine the possible influence of the lipid structure on lipase activity in the aerosol environment pertaining to the specific type of lipid head group and the degree of saturation in side chains: triolein and linolein contain three oleic acid [18:1 (9Z)] and three linoleic acid [18:2 (9Z, 12Z)] side chains, respectively, while PE-dioleoyl have two oleic acid side chains and one phosphatidylethanolamine head group attached to the backbone. As a glycerol ester hydrolase, lipase cleaves only the ester bonds in the lipids allowing the corresponding fatty acid to be detected. Typical negative-ion mode mass spectra recorded after triolein and PE-dioleoyl lipids were separately exposed to lipase (1:1 mole ratio, 25 μM) are shown in Figure 2B,C, respectively. High abundance of the expected oleic acid reaction product was detected in both cases at m/z 281. Although the lipid solutions were prepared in pure chloroform and the lipase in water, the enzymatic reaction product was detected instantaneously after the two solutions were brought together in the droplet phase. This signifies remarkable interfacial and/or rapid mixing effects in the droplet environment, allowing the lipids to gain access to the active site of the enzyme despite solution immiscibility. Unlike triolein, the acidic phosphate head group in PE-dioleoyl (denoted M) enabled detection of the intact lipid as (M − H), at m/z 742

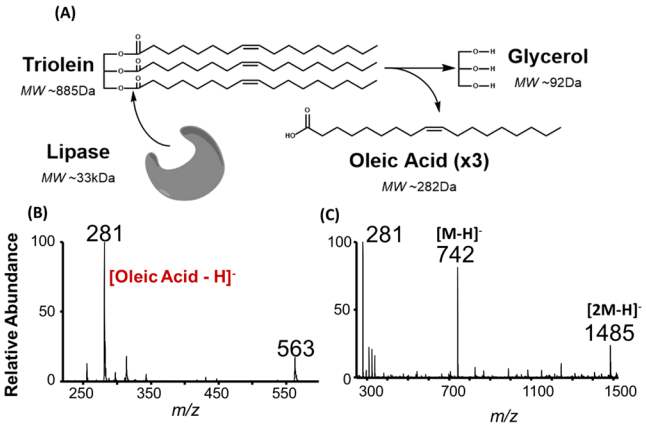

Figure 2. (A) Schematic illustrating the hydrolytic action of lipase on lipids. The reaction proceeds in a stepwise fashion that yields three free fatty acid molecules and a glycerol molecule at the end of the reaction. Similar schematic is shown in Figure S5 for other reactions. Using triolein as an example, which produces oleic acid (MW 282 Da), typical negative-ion mode mass spectra were recorded after exposing (B) triolein (MW 885 Da) and (C) PE-dioleoyl (M, MW 743 Da) separately to lipase in the charged microdroplet environment in real time using the contained-ES apparatus operated in the type II mode (cavity length 10 mm). Peak at m/z 563 in panel (B) is a dimer of oleic acid, with tandem MS data shown in Figure S6 in the Supporting Information.

(Figure 2C), which was accompanied by the dimeric species at m/z 1485. We determined that for triolein, the corresponding equilibrium bulk-phase reaction required at least 14 min to generate comparable oleic acid yield (Figure S2). Similar observations were made for the enzyme-catalyzed hydrolysis of PE-dioleoyl and linolein where a minimum of 6 min was required for the solution-phase biphasic reaction to produce comparable yields as the droplet reactions (Figures S3 and S4).

Previous studies have shown increased droplet reactivity with increased flight distance due to solvent evaporation, which leads to concentration and surface effects.[35−40] Similar observations have recently been made with the contained-ES apparatus even at short analytical spray distances (<5 mm),[30,31] making it possible to accurately examine the kinetics of lipase hydrolysis using known droplet velocities to convert the cavity length to reaction time. This required important control experiments to enable correct interpretation of data. These included accessing the stability of the lipid in organic solution and in the presence of water and high electric field, as well as the stability of lipase enzyme under similar conditions. As shown in Figure 3A for triolein hydrolysis, a significant amount of oleic acid was produced only when the lipid and lipase were sprayed together coaxially in either type I or II operation modes. Similar results were observed for linolein and PE-dioleoyl (Figures S7 and S8) in which the lipids registered great stability in the absence of the lipase enzyme in the charged microdroplet environment. Comparing different cavity lengths, it is apparent that the reaction progresses more effectively as the reagent's residence time in the cavity increased. The ion intensities of the fatty acids generated from the enzymatic reaction were converted to molar concentrations through external calibration (see Figure 3B for regression line obtained using standard concentrations of oleic acid). We used external calibration to ensure that unwanted effects due to backward reactions[41,42] between free fatty acid and lipase are minimized. Consequently, we were

https://doi.org/10.1021/acs.analchem.1c02785
Anal. Chem. 2021, 93, 13001−13007

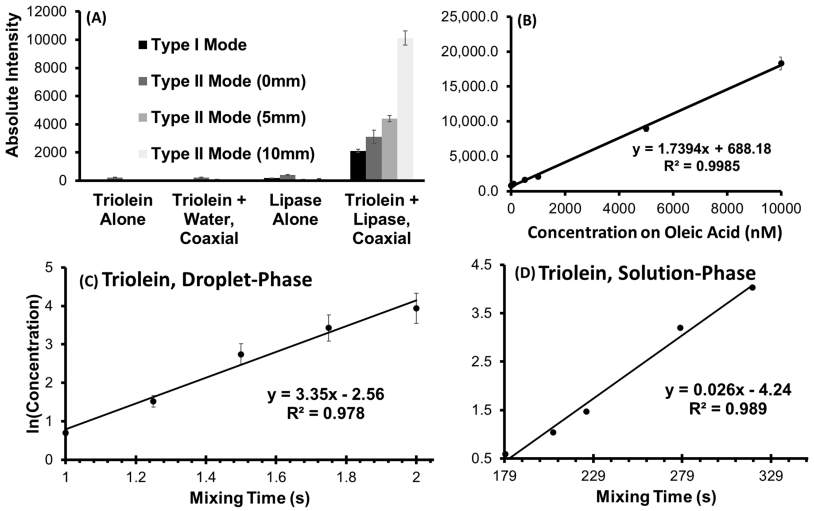

Figure 3. (A) Absolute ion (M − H)—intensities of oleic acid produced from triolein after exposure to lipase under different spray conditions (type I and type II, cavity lengths 1, 5, 10 mm) are compared to the signal derived from various control experiments: triolein alone, coaxial spray of triolein in chloroform and pure water containing no lipase enzyme, and lipase alone. (B) Calibration curve for oleic acid using (M − H)—ion signal versus solution-phase concentration. Linearized data showing the concentration of oleic acid produced as a result of lipase-catalyzed hydrolysis of triolein, as a function of reaction time when reactions were performed under (C) droplet-phase and (D) solution-phase conditions.

able to quantify product formation in the droplet environment as a function of time (Figure 3C). *Note*: the actual concentration versus time plots showed exponential curves, as would be expected for the pseudo-first-order enzymatic reaction[43] (Figures S9−S11). Therefore, the logarithmic function is used here to generate this straight line presented for triolein hydrolysis by lipase. (The slopes for the raw exponential data are unaffected by the linearization process.) We then performed similar rate measurements using bulk-solution-phase reaction conditions (Figure 3D) and compared the rate constants (i.e., slopes in mol/L/s) of the two curves, which represents the enhancement factor for the droplet-based reaction. The rate constants and associated enhancement factors are summarized in Table 1 for all lipids tested. In all cases, we observed more than 2 orders of magnitude increase in enzymatic activity in the droplet environment compared with bulk-solution phase. This is not surprising given that, due to immiscibility, the bulk-phase enzymatic reactions occurred at the interface between the aqueous lipase solution and chloroform solution of the lipids. The droplet system offers much more interfacial contact due to the increased surface area of the tiny droplets generated in the reaction cavity. This interpretation is consistent with previous reports that demonstrated highly efficient lipase catalysis in micro-emulsions.[44,45]

Table 1. Comparison of Rate Constants of Lipase-Catalyzed Lipid Hydrolysis between Droplet-Phase and Solution-Phase Reactions[a]

		rate constant (mol/L/s)		
#	lipid	droplet	bulk ($\times 10^{-2}$)	E-factor[b]
1	triolein (ideal, pH 7)	3.60 ± 0.01	2.6 ± 0.47	138
2	triolein (environmental, pH 8)	3.89 ± 0.63	0.4 ± 0.074	972
3	linolein (ideal, pH 7)	5.64 ± 0.19	2.0 ± 0.37	282
4	PE-dioleoyl (ideal, pH 7)	6.71 ± 0.50	2.8 ± 0.32	239
5	PE-dioleoyl (miscible solvents)	2.39 ± 0.40	1.4 ± 0.30	171

[a]The associated enhancement factors are provided in favor of the droplet chemistry. Ideal experiments involved pure aqueous lipase solution, while the environmental experiment was performed using Tris−EDTA buffered solution. [b]Enhancement (E) factor.

Reaction Time Dependence on Cavity Size. The type I operation mode (i.e., ES emitters extend beyond the outer capillary by approximately 2.5 mm) mixes reactants rapidly in moving droplets in air. With the spray distance (distance between the tip of the outer capillary of the contained-ES apparatus to the inlet of mass spectrometer) kept at 10 mm, mixing times of only milliseconds are allowed under this spray condition and yet good enzymatic activity is observed (Figure 3A). Enzymatic activity is observed to further increase in the droplet environment when the electrospray emitters were pulled inside the outlet of the contained-ES source by only 1 mm in the type II operation mode (i.e., cavity length was kept at 1 mm). The presence of the reaction cavity induces strong turbulent mixing[31] that facilitates reactions. We have also observed the existence of liquid thin films in the cavity that are sprayed along the walls of the outer capillary, which then give rise to microdroplets. Both the microdroplets and the thin liquid films are well-known microreactors that can enhance enzymatic reactions. Most importantly, concentration effects contribute to the observed rate enhancement. This is established by the continuous delivery of reagents into the cavity following solvent evaporation from the initial droplets collected inside the cavity, resulting in the formation of a discontinuous thin film in which the volume of the arriving droplets is compensated for by the evaporative loss of the solvent due to fast N_2 nebulizing gas flow.[31] It is important to note that the droplets we monitored for enzymatic activity are derived from the thin film. Thus, the chemical content of the droplets is expected to be similar to the thin film precursor, allowing the reaction to continuously progress in the cavity.

Careful inspection of rate constant data for the different lipids in bulk-solution phase revealed only modest differences in the enzymatic activity, where 2.0×10^{-2}, 2.6×10^{-2}, and 2.8×10^{-2} mol/L/s were recorded for linolein, triolien, and PE-

https://doi.org/10.1021/acs.analchem.1c02785
Anal. Chem. 2021, 93, 13001−13007

dioleoyl, respectively. Although small, the decrease in lipase activity from triolien to linolein is consistent with previous reports that showed that lipases become less effective as the number of double bonds in the side chain of the lipid is increased.[46,47] This order is reversed for the droplet experiment where a significantly higher rate constant (5.64 mol/L/s) is measured for linolein compared with 3.60 mol/L/s for triolien. Therefore, we believe that molecular cross section and solubility are other contributing factors. With linolein having a higher molecular cross section than triolein (145×10^{-16} cm^2 per molecule),[48] linolein can be expected to pack less efficiently at the interface leading to a fewer number of molecules and hence less efficient production of linoleic acid under the solution-phase reaction condition. For the droplet-phase experiments, interfacial contacts between the individual immiscible droplets take precedence over packing density since the lipase enzyme and the lipid, though both are surface-active, cannot share the same space on the surface of the microdroplet. On the other hand, enzymatic reactions occurring within a single microdroplet will be governed by the solubility of the lipid. Theoretical computations to determine aqueous solubility were run using the ALOGPS program, and the solubility of linolein in water was calculated to be 7.84×10^{-6} g/L, which is slightly larger than the solubility of triolein in water (6.13×10^{-6} g/L). In smaller microdroplet volumes, this difference in solubility can result in a large difference in concentration, which can subsequently lead to a markedly different product yield. Preferential hydrolysis of linolein by lipase in the droplet environment was further investigated. We used a solution containing equimolar mixture of linolein and triolein, which was sprayed and exposed to lipase in the droplet phase. The rate constant for linolein in the mixture was calculated to be 4.61 ± 0.21 mol/L/s, (Figure S12), which was slightly higher than the rate constant recorded for triolein (4.05 ± 0.26 mol/L/s). This result is consistent with the individual lipid hydrolytic reactions where a higher rate constant was observed for linolein compared to that for triolein in the droplet environment (Table 1). The slight differences in the rate constants may reflect the competitive nature of hydrolysis when using a solution containing both lipids. The insight on the effect of solubility is supported by considering PE-dioleoyl (solubility in water 6.19×10^{-5} g/L), which has a polar head group. Although PE-dioleoyl has only two oleic acid molecules in the side chain, its solubility in water is an order of magnitude greater than that for triolein and linolein, accounting for the reason why the enzymatic rate constants are higher for PE-dioleoyl (entry #4, Table 1) in both bulk-solution-phase and droplet-phase reaction conditions. Solubility may be further improved in the droplet environment due to possible micelle formation as indicated by the presence of high-order lipid clusters during the electrospray (Figure S13).

Replicating Relevant Conditions. We sought to increase the complexity of the systems by preparing the lipase in the Tris−EDTA buffer solution (pH 8 and 100 nM lipase). This buffer solution emulates the pH of ocean water. Triolein in pure chloroform was used, which was prepared at a 5 μM concentration. The two solutions were sprayed coaxially using the contained-ES apparatus in the type II operation mode with varying cavity length, and the rates of oleic acid production were compared to those derived from solution-phase reaction conditions (entry #2, Table 1). Like the earlier systems, the rate curve for the Tris−EDTA buffered lipase solution followed an exponential model (Figure S14), and the data were similarly linearized (Figure S15). Comparison of rate constants of these buffered conditions showed an enhancement factor of almost 103 in favor of the droplet-phase reaction condition. When compared with the ideal system (entry #1, Table 1), the greater enhancement factor observed for the buffered system can be ascribed to a decrease in rate constants from 2.6×10^{-2} to 0.4×10^{-2} mol/L/s, respectively, for solution-phase reaction conditions and the concomitant increase in rate constant in the droplet reaction conditions, from 3.6 mol/L/s in that case of ideal solution to 3.9 mol/L/s for the buffered system. The significant decrease in product yield for buffered solution-phase reaction condition may be related to the presence of interfering species that can occupy the active site of the enzyme and hinder its activity toward the lipid (the disodium EDTA species are present at 1 mM levels, which is approximately 200× more concentrated than triolein). However, when the same complex solution is electrosprayed before mixing with triolein in the droplet phase, the reduced volume leads to a decrease in the number of EDTA molecules in the microdroplets,[49] allowing more access to the active site of the enzyme via a more efficient interfacial contact due to increased surface area. Also, the buffered solution prevents extreme pH changes in the droplet environment that can have detrimental effects on enzyme activity. Collectively, these results reveal that the specific chemical composition of marine aerosols after ejection from the ocean surface can sustain enzymatic reactions more favorably than reactions occurring in the SSML. The enhancement factor recorded for droplets derived from the buffered lipase solution is approximately 1 order of magnitude higher than the values obtained for coastal marine aerosols.[17−19] The difference could be attributed to the fact that the marine aerosols are far more complex than droplets generated from the Tris−EDTA solution using the contained-ES apparatus. However, it is also possible that the typical analysis method, where the collected aerosols are reconstituted into solution, may not represent the true activity of enzymes in the atmosphere.

Mechanistic Considerations. The atmospheric implications of this study derive from the mechanistic insights obtained based on solubility and interfacial parking and interactions. Two mechanisms are identified that could enable large proteins/enzymes trapped in aerosols to react with their substrates in the atmosphere: in-aerosol reactions facilitated by solubility and interfacial reactions occurring between two individual aerosols coalescing in air (Scheme 1). Unlike SSML, it is unreasonable to presume that lipase will be able to insert itself into the thin lipid layer at the aerosol surface; both molecules cannot occupy the exact space at the droplet surface. For lipids with higher water solubility (e.g., PE-dioleoyl),

Scheme 1. Possible Mechanisms of Enzymatic Reactions in Droplet Environment: (A) Reactions Occurring Inside the Bulk of the Droplet Due to the High Solubility of the Lipid and (B) Droplet−Droplet Interfacial Reactions Enabled through Droplet Coalescence

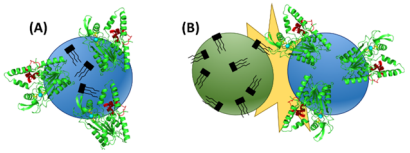

https://doi.org/10.1021/acs.analchem.1c02785
Anal. Chem. 2021, 93, 13001−13007

enzyme-catalyzed hydrolysis may occur inside the aerosol where the lipase and the soluble lipid may be trapped, as illustrated in Scheme 1A. On the other hand, a possible mechanism for sparingly soluble lipids may involve droplet−droplet interfacial reactions, with the lipid residing at the surface one droplet and active site of lipase exposed at the second droplet (Scheme 1B). To investigate the validity of coexistence of these distinct mechanisms for enzymatic reaction, we performed experiments using miscible systems (PE-dioleoyl in 1:2 chloroform:methanol, lipase in 1:1 methanol/water). We expect such miscible solvents to hinder interfacial effects and consequently change reaction rate significantly if interfacial interactions are important. Indeed, the rate constant reduced from 6.71 ± 0.5 mol/L/s (for immiscible systems with interfacial effects; entry #4, Table 1) to 2.39 ± 0.4 mol/L/s (for the miscible solvent system; entry #5, Table 1 and Figures S16 and S17). This result represents a significant reduction in reaction rate confirming the importance of interfacial droplet−droplet interactions in atmospheric chemistry.

CONCLUSIONS

Overall, aerosol proxies were created using contained-electrospray ionization and enzymatic activity in the aerosol studied using mass spectrometry in real time. The lipase enzyme showed great stability in the presence of an electric field during electrospray and in the presence of chloroform in which the lipid solutions were prepared. The novel coaxial spray mode with reaction cavity provided efficient means to react chemical species in two immiscible solutions and to monitor product yield as a function of time. While the rate constants obtained for lipase-catalyzed hydrolysis of glyceryl trioleate, glyceryl trilinoleate, and L-α-phosphatidylethanolamine dioleoyl in solution phase varied only slightly (0.020−0.028 mol/L/s), large differences in rate constants were observed for the droplet-phase experiment, ranging from 3.4 to 6.3 mol/L/s. This indicates that small differences in chemical properties such as solubility, parking density, and surface activities can have large effects in the small-volume droplet environment and result in significant enhancements in chemical reactions. In particular, the study shows that lipase retained activity in charged microdroplets and caused the hydrolysis of all lipids tested on a millisecond timescale (type I spray mode). The enhanced aerosol reactivity can have profound implications in atmospheric chemistry.

ASSOCIATED CONTENT

Supporting Information

The Supporting Information is available free of charge at https://pubs.acs.org/doi/10.1021/acs.analchem.1c02785.

Pertaining to the use of chloroform as a spray solvent; various mass spectra of lipid and fatty acid modifications; and nonlinearized (raw) and linearized data are provided for all subject lipids of this study, including improved miscibility and competition studies (PDF)

AUTHOR INFORMATION

Corresponding Author

Abraham K. Badu-Tawiah − *Department of Chemistry and Biochemistry, The Ohio State University, Columbus, Ohio 43210, United States;* orcid.org/0000-0001-8642-3431; Email: badu-tawiah.1@osu.edu

Author

Benjamin J. Burris − *Department of Chemistry and Biochemistry, The Ohio State University, Columbus, Ohio 43210, United States*

Complete contact information is available at: https://pubs.acs.org/10.1021/acs.analchem.1c02785

Author Contributions

The manuscript was written through contributions of all authors. All authors have given approval to the final version of the manuscript.

Notes

The authors declare no competing financial interest.

ACKNOWLEDGMENTS

This work was supported by the National Science Foundation (Award No. CHE-1900271) and through the NSF Center for Aerosol Impacts on Chemistry of the Environment (CAICE; Award No. CHE-1801971).

REFERENCES

(1) Cunliffe, M.; Upstill-Goddard, R. C.; Murrell, J. C. *FEMS Microbiol. Rev.* **2011**, *35*, 233−246.
(2) Fuhrman, J.; Sleeter, T.; Carlson, C.; Proctor, L. *Mar. Ecol.: Prog. Ser.* **1989**, *57*, 207−217.
(3) Reinthaler, T.; Sintes, E.; Herndl, G. J. *Limnol. Oceanogr.* **2008**, *53*, 122−136.
(4) Wurl, O.; Holmes, M. *Mar. Chem.* **2008**, *110*, 89−97.
(5) Engel, A.; Galgani, L. *Biogeosciences* **2016**, *13*, 989−1007.
(6) Sieburth, J. M. In Air-Sea Exchange of Gases and Particles. In *NATO ASI Series (Series C: Mathematical and Physical Sciences)*;Liss, P. S.; Slinn, W. G. N., Eds.; Springer, Dordrecht, 1983; Vol. *108*, pp 121−172.
(7) Cunliffe, M.; Salter, M.; Mann, P. J.; Whiteley, A. S.; Upstill-Goddard, R. C.; Murrell, J. C. *FEMS Microbiol. Lett.* **2009**, *299*, 248−254.
(8) Kuznetsova, M.; Lee, C. *Mar. Chem.* **2001**, *73*, 319−332.
(9) Mustaffa, N. I. H.; Striebel, M.; Wurl, O. *Geophys. Res. Lett.* **2017**, *44*, 12324−12330.
(10) Cramer, K. L.; O'Dea, A.; Clark, T. R.; Zhao, J.; Norris, R. D. *Nat. Commun.* **2017**, *8*, No. 14160.
(11) Mayol, E.; Jiménez, M. A.; Herndl, G. J.; Duarte, C. M.; Arrieta, J. M. *Front. Microbiol.* **2014**, *5*, No. 557.
(12) Reche, I.; D'Orta, G.; Mladenov, N.; Winget, D. M.; Suttle, C. A. *ISME J.* **2018**, *12*, 1154−1162.
(13) Cochran, R. E.; Ryder, O. S.; Grassian, V. H.; Prather, K. A. *Acc. Chem. Res.* **2017**, *50*, 599−604.
(14) DeMott, P. J.; Hill, T. C. J.; McCluskey, C. S.; Prather, K. A.; Collins, D. B.; Sullivan, R. C.; Ruppel, M. J.; Mason, R. H.; Irish, V. E.; Lee, T.; Hwang, C. Y.; Rhee, T. S.; Snider, J. R.; McMeeking, G. R.; Dhaniyala, S.; Lewis, E. R.; Wentzell, J. J. B.; Abbatt, J.; Lee, C.; Sultana, C. M.; Ault, A. P.; Axson, J. L.; Diaz Martinez, M.; Venero, I.; Santos-Figueroa, G.; Stokes, M. D.; Deane, G. B.; Mayol-Bracero, O. L.; Grassian, V. H.; Bertram, T. H.; Bertram, A. K.; Moffett, B. F.; Franc, G. D. *Proc. Natl. Acad. Sci. U.S.A.* **2016**, *113*, 5797−5803.
(15) Estillore, A. D.; Trueblood, J. V.; Grassian, V. H. *Chem. Sci.* **2016**, *7*, 6604−6616.
(16) Ault, A. P.; Guasco, T. L.; Baltrusaitis, J.; Ryder, O. S.; Trueblood, J. V.; Collins, D. B.; Ruppel, M. J.; Cuadra-Rodriguez, L. A.; Prather, K. A.; Grassian, V. H. *J. Phys. Chem. Lett.* **2014**, *5*, 2493−2500.
(17) Collins, D. B.; Ault, A. P.; Moffet, R. C.; Ruppel, M. J.; Cuadra-Rodriguez, L. A.; Guasco, T. L.; Corrigan, C. E.; Pedler, B. E.; Azam, F.; Aluwihare, L. I.; Bertram, T. H.; Roberts, G. C.; Grassian, V. H.; Prather, K. A. *J. Geophys. Res.: Atmos.* **2013**, *118*, 8553−8565.

(18) Wang, X.; Sultana, C. M.; Trueblood, J.; Hill, T. C. J.; Malfatti, F.; Lee, C.; Laskina, O.; Moore, K. A.; Beall, C. M.; McCluskey, C. S.; Cornwell, G. C.; Zhou, Y.; Cox, J. L.; Pendergraft, M. A.; Santander, M. V.; Bertram, T. H.; Cappa, C. D.; Azam, F.; DeMott, P. J.; Grassian, V. H.; Prather, K. A. *ACS Cent. Sci.* **2015**, *1*, 124−131.
(19) Collins, D. B.; Bertram, T. H.; Sultana, C. M.; Lee, C.; Axson, J. L.; Prather, K. A. *Geophys. Res. Lett.* **2016**, *43*, 9975−9983.
(20) Malfatti, F.; Lee, C.; Tinta, T.; Pendergraft, M. A.; Celussi, M.; Zhou, Y.; Sultana, C. M.; Rotter, A.; Axson, J. L.; Collins, D. B.; Santander, M. V.; Anides Morales, A. L.; Aluwihare, L. I.; Riemer, N.; Grassian, V. H.; Azam, F.; Prather, K. A. *Environ. Sci. Technol. Lett.* **2019**, *6*, 171−177.
(21) Jimenez, J. L. J. *J. Geophys. Res.* **2003**, *108*, No. 8425.
(22) Prather, K. A.; Nordmeyer, Trent.; Salt, Kimberly. *Anal. Chem.* **1994**, *66*, 1403−1407.
(23) Schmid, R. D.; Verger, R. *Angew. Chem., Int. Ed.* **1998**, *26*, 1608−1633.
(24) Schrag, J. D.; Li, Y.; Cygler, M.; Lang, D.; Burgdorf, T.; Hecht, H.-J.; Schmid, R.; Schomburg, D.; Rydel, T. J.; Oliver, J. D.; Strickland, L. C.; Dunaway, C. M.; Larson, S. B.; Day, J.; McPherson, A. *Structure* **1997**, *5*, 187−202.
(25) Bakhtiari, M.; Konermann, L. *J. Phys. Chem. B* **2019**, *123*, 1784−1796.
(26) Katta, V.; Chait, B. T. *J. Am. Chem. Soc.* **1991**, *113*, 8534−8535.
(27) Konermann, L.; Ahadi, E.; Rodriguez, A. D.; Vahidi, S. *Anal. Chem.* **2013**, *85*, 2−9.
(28) Kulyk, D. S.; Miller, C. F.; Badu-Tawiah, A. K. *Anal. Chem.* **2015**, *87*, 10988−10994.
(29) Kulyk, D. S.; Sahraeian, T.; Wan, Q.; Badu-Tawiah, A. K. *Anal. Chem.* **2019**, *91*, 6790−6799.
(30) Miller, C. F.; Kulyk, D. S.; Kim, J. W.; Badu-Tawiah, A. K. *Analyst* **2017**, *142*, 2152−2160.
(31) Miller, C.; Burris, B.; Badu-Tawiah, A. K. *J. Am. Soc. Mass Spectrom.* **2020**, *31*, 1499−1508.
(32) Sahraeian, T.; Kulyk, D. S.; Badu-Tawiah, A. K. *Langmuir* **2019**, *35*, 14451−14457.
(33) Venter, A.; Sojka, P. E.; Cooks, R. G. *Anal. Chem.* **2006**, *78*, 8549−8555.
(34) Liu, R. H.; Stremler, M. A.; Sharp, K. V.; Olsen, M. G.; Santiago, J. G.; Adrian, R. J.; Aref, H.; Beebe, D. J. *J. Microelectromech. Syst.* **2000**, *9*, 190−197.
(35) Lee, J. K.; Kim, S.; Nam, H. G.; Zare, R. N. *Proc. Natl. Acad. Sci. U.S.A.* **2015**, *112*, 3898−3903.
(36) Zhong, X.; Chen, H.; Zare, R. N. *Nat. Commun.* **2020**, *11*, No. 1049.
(37) Yan, X.; Bain, R. M.; Cooks, R. G. *Angew. Chem., Int. Ed.* **2016**, *55*, 12960−12972.
(38) Lee, J. K.; Banerjee, S.; Nam, H. G.; Zare, R. N. *Q. Rev. Biophys.* **2015**, *48*, 437−444.
(39) Banerjee, S.; Gnanamani, E.; Yan, X.; Zare, R. N. *Analyst* **2017**, *142*, 1399−1402.
(40) Zhao, P.; Gunawardena, H. P.; Zhong, X.; Zare, R. N.; Chen, H. *Anal. Chem.* **2021**, *93*, 3997−4005.
(41) Rogalska, E.; Ransac, S.; Verger, R. *J. Biol. Chem.* **1990**, *265*, 20271−20276.
(42) Johnson, K. A. *J. Biol. Chem.* **2008**, *283*, 26297−26301.
(43) Schnell, S.; Mendoza, C. *Biophys. Chem.* **2004**, *107*, 165−174.
(44) Stamatis, H.; Xenakis, A.; Kolisis, F. N. *Biotechnol. Adv.* **1999**, *17*, 293−318.
(45) Reis, P.; Miller, R.; Leser, M.; Watzke, H. *Appl. Biochem. Biotechnol.* **2009**, *158*, 706−721.
(46) Raclot, T.; Holm, C.; Langin, D. *J. Lipid Res.* **2001**, *42*, 2049−2057.
(47) Kraemer, F. B.; Shen, W.-J. *J. Lipid Res.* **2002**, *43*, 1585−1594.
(48) Langmuir, I. *Proc. Natl. Acad. Sci. U.S.A.* **1917**, *3*, 251−257.
(49) Susa, A. C.; Xia, Z.; Williams, E. R. *Angew. Chem., Int. Ed.* **2017**, *56*, 7912−7915.

https://doi.org/10.1021/acs.analchem.1c02785
Anal. Chem. 2021, 93, 13001−13007